Organic Electronics 12 (2011) 1137–1141

Contents lists available at ScienceDirect

Organic Electronics

journal homepage: www.elsevier.com/locate/orgel

High-color-rendering flexible top-emitting warm-white organic light emitting diode with a transparent multilayer cathode

Wenyu Ji [a,b,*], Jialong Zhao [a], Zaicheng Sun [a], Wenfa Xie [b,*]

[a] Key Laboratory of Excited State Processes, Changchun Institute of Optics, Fine Mechanics and Physics, Chinese Academy of Sciences, Changchun 130033, People's Republic of China

[b] State Key Laboratory on Integrated Optoelectronics, College of Electronic Science and Engineering, Jilin University, Changchun 130012, People's Republic of China

ARTICLE INFO

Article history:
Received 28 January 2011
Received in revised form 15 March 2011
Accepted 28 March 2011
Available online 9 April 2011

Keywords:
OLEDs
Multilayer
Phase
Transparent
Color-rendering index

ABSTRACT

A top-emitting warm-white organic light emitting diode (TEWOLED) was fabricated with a conductive transparent MAM cathode [MAM = MoO_3 (40 nm)/Ag (17 nm)/MoO_3 (40 nm)], which had a higher color rendering index (CRI) than that of corresponding ITO-based bottom-emitting organic light-emitting device (OLED). We measured and calculated the optical transmittance of multilayer MAM fabricated on PET substrate by vacuum thermal evaporation. The average transmittance in visible range is above 84%, which is similar to the conventional indium tin oxide (ITO). The weak microcavity effect on the device performance was also studied. MAM multilayer has the potential for using as transparent conductor electrodes for white OLEDs, especially for flexible devices due to its unique optical and electrical properties.

© 2011 Elsevier B.V. All rights reserved.

1. Introduction

White organic light emitting diode (WOLEDs) are of interest recently due to their potential use in full-color flat-panel displays and low power consumption solid state lighting sources [1–7]. As lighting sources, TEWOLEDs will be superior to bottom-emitting OLEDs because they can be fabricated on opaque and flexible substrates, such as metal foils and plastics, replacing rather expensive glass substrates coated with indium tin oxide (ITO). In addition, TEWOLEDs combined with red, green, and blue color filters and driving circuit, such as organic thin film transistor (OTFT) [8–10] and complementary metal oxide semiconductor (CMOS) [11–13], are the most effective method to obtain high-resolution displays due to a high aperture ratio in active matrix OLEDs. However, due to the strong microcavity effects, it remains a challenge to generate white light in top-emitting devices. Especially, TEWOLEDs with high color rendering index (CRI) are hardly achieved. Thus, extensive efforts have focused on eliminating the microcavity effect in TEWOLEDs [14–16]. Besides, the TEWOLEDs utilizing microcavity effect [17–19], down-conversion phosphors [20] were also reported. But all the reported TEWOLEDs have some disadvantages, such as the use of active metal calcium [14], sputtering deposition process for ITO [15], the low CRI [17–20] and efficiency [16,20]. In order to achieve advanced performance, one of the strategies is to use high transmittance top electrode in TEWOLEDs. Due to the rising cost of indium, brittleness, need for high growth temperature and special technology, and the diffusion nature of indium ions which is harmful to the long-term performance of OLEDs, the currently used ITO has significant shortcomings for low-cost, large-area, and flexible device applications [21,22]. An alternative to ITO as transparent conductors is the use of dielectric/metal/dielectric (D/M/D) multilayer, which suppresses the reflection of the metal layer and achieves selective high transparent effect [23]. In 1998, Bender et al. reported

* Corresponding authors at: Key Laboratory of Excited State Processes, Changchun Institute of Optics, Fine Mechanics and Physics, Chinese Academy of Sciences, Changchun 130033, People's Republic of China (W. Ji).

E-mail addresses: jlujwy@gmail.com, xiewf@jlu.edu.cn (W. Ji).

1566-1199/$ - see front matter © 2011 Elsevier B.V. All rights reserved.
doi:10.1016/j.orgel.2011.03.042

ITO/Ag/ITO (IMI) structure with higher conductivity [24]. Recently, Lewis et al. reported flexible OLEDs based on IMI stacks which fabricated onto polyethylene terephthalate (PET) by sputtering deposition process [22]. In addition, multilayer InZnSnOx/Ag/InZnSnOx, ZnS/Ag/ZnS, WO_3/Ag/WO_3, and ITO/Ag/WO_3 were also reported as electrodes for OLEDs [25–28]. But all the reported multilayer electrodes above were almost used in monochrome OLEDs, having no white light emission devices reported.

In this article, we reported a warm and high color-rendering TEWOLED with MoO_3/Ag/MoO_3 (MAM) multilayer used as a cathode. We prepared conductive transparent MAM coating on PET substrates by vacuum thermal evaporation and measured the optical transmittance. The TEWOLED we fabricated had a comparable efficiency but superior CRI relative to bottom-emitting OLED.

2. Experimental details

The device A consisted of PET substrate/Al (100 nm)/MoO_3 (1.5 nm)/4, 4′, 4″-tris(3-methylphenyl–phenylamino)-tripheny-lamine (m-MTDATA, 30 nm)/N, N′-bis-(1-naphthyl)-N, N'diphenyl-1, 1-biphenyl-4, 4′diamine (NPB, 10 nm)/4, 4′-bis(2, 2′-diphenylvinyl)-1, 1′-biphenyl (DPVBi, 15 nm)/4, 4-N, N- dicarbazole-biphenyl (CBP, 3 nm)/CBP: bis(2-(2-fluorphenyl)-1, 3-benzothiozolato-N, C2′)iridium(acetylacetonate) [(F–BT)2Ir(acac)] (7 nm)/4, 7-diphenyl -1, 10-phenanthroline (Bphen, 30 nm)/LiF (1 nm)/Al (1 nm)/Ag (1 nm)/MoO_3 (40 nm)/Ag (17 nm)/MoO_3 (40 nm). In this device, Al/MoO_3, m-MTDATA, NPB, DPVBi, CBP: $(F–BT)_2Ir(acac)$, Bphen, and LiF/Al/Ag/M/A/M were used as the anode, hole injection layer, hole transporting layer, blue emitting layer, orange emitting layer, electron transporting layer and cathode, respectively. Here, we use metal Al as the anode replacing the common metal Ag because Al film has larger phase shift on reflection than that of metal Ag. The neat CBP is introduced to separate blue and orange emitting layers to avoid the Dexter energy transfer between the two emitters. For comparison, the bottom-emitting device (ITO glass substrate) with the same organic layers (device B) was fabricated, which consisted of glass coated with ITO /m-MTDATA (30 nm)/NPB (10 nm)/DPVBi (15 nm)/CBP (3 nm)/CBP: $(F–BT)_2Ir(acac)$ (7 nm)/Bphen (30 nm)/LiF (1 nm)/Al (200 nm). All films were deposited at pressure below 4×10^{-6} Torr. The deposition of each layer and the measure of devices characteristics were described before [20].

3. Results and discussion

Ryu et al. reported that the Ag thin film was the dominant factor of the sheet resistance in a dielectric/Ag/dielectric multilayer [28]. Consequently, a low resistance of multilayer cathode will be obtained by adjusting the thickness of Ag layer in MAM electrode. We measured the sheet resistance of the prepared MAM multilayer by four-point probe and a low resistance of 11 Ω/□ was obtained. If the film boundary effects are negligible, the sheet resistance of the multilayer is the sheet resistance of MoO_3, Ag, MoO_3 layer coupled in parallel: [28].

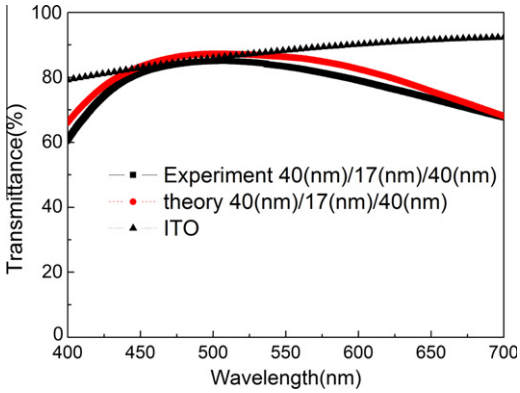

Fig. 1. The measured optical transmittance curves of MAM and ITO, the calculated optical transmittance of MAM is also plotted.

$$\frac{1}{R_{total}} = \frac{1}{R_{MoO3}} + \frac{1}{R_{Ag}} + \frac{1}{R_{MoO3}}.$$

R_{total}, R_{Ag}, R_{MoO3} is the sheet resistance of MAM, Ag, MoO_3 layer, respectively. Fig. 1 shows the measured and calculated optical transmittance curves of multilayer MAM as a function of the wavelength. The optical transmittance is calculated by the transfer-matrix method [29]. The measured optical transmittance curve of ITO was also plotted in Fig. 1. It can be seen that a high average transmittance of over 84% is obtained for the MAM-based transparent multilayer, which is comparable with the conventional ITO. Here, we also calculated the transmittance of MoO_3 (y nm)/Ag (17 nm)/MoO_3 (y nm) for different y value (the data was not shown) and found that the MAM multilayer had the highest transmittance when $y = 40$. Considering the electric and optical properties, we choose a 17 nm Ag layer for MAM coating. One should note that the MAM multilayer with superior features is obtained by simple thermal evaporation without subjecting to substrate heating and post-annealing, which is especially favorable for flexible OLEDs and top-emitting OLEDs.

Fig. 2a shows the normalized EL spectra of device A and B at operating voltage of 6, 8, and 10 V. It can be seen that the narrowness of the full width at half maximum (FWHM) of the DPVBi and $(F\text{-}BT)_2Ir(acac)$ emission in device A is not observed at all. Insert is the normal spectra normalized to blue emission. We can see that the devices have the same blue emission spectral profile. However, the spectra have large difference in long wavelength region. In order to explain this, we calculated the phase shift characteristics of the TEWOLED by the transfer-matrix method [29], as shown in Fig. 2b, the calculated round-trip phase changes for organic layers sandwiched between two reflection electrodes [i.e., $\varphi_1(\lambda) = \sum_i \frac{4\pi d_i n_i(\lambda)}{\lambda}$], and the phase changes at two reflective electrodes [i.e., $\varphi_2(\lambda) = \varphi_{cathode} + \varphi_{anode}$]. In our calculation, the multilayer MoO_3 (40 nm)/Ag (17 nm)/MoO_3 (40 nm) was considered the cathode. The point of intersection is the resonant wavelength (RW). It can be seen that a RW at 635 nm is observed. Insert is the absorptance and reflectance of multilayer MAM. The absorptance is almost the same over the visible range, which will not affect the distribution of the spectrum intensity. High reflectance (>25%) at longer wavelength (>600 nm) will benefit

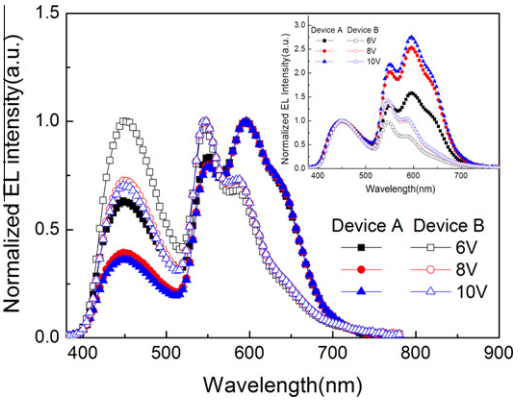

Fig. 2a. The normalized EL spectra of devices A and B at different voltage of 6, 8, and 10 V; Insert is the EL spectra of devices A and B normalized to blue emission.

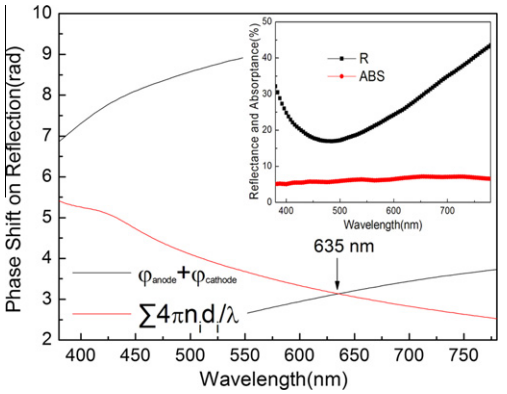

Fig. 2b. The calculated round-trip phase changes for 95 nm organic layers between two electrodes and the phase changes on two electrodes for normal incidence; Insert is the calculated optical reflectance and absorptance curves of MAM coating.

to the light emission near 635 nm due to constructive interference. High reflectance at shorter wavelength would attenuate the blue emission intensity near 439 nm where the destructive interference arises. In order to clarify the microcavity effect in the device, we calculated the cavity emission by considering wavelength-independment instrsinc luminescence spectra of the emitters [30], as shown in Fig. 2c. The calculated resonant wavelength of the device is 638 nm, which is agreement with the calculated result for the phase shift. We can see that the cavity emission is varied with wavelength, which will result in a different enhanced emission st different wavelength for device A. Thus, device A shows a more enhanced orange emission and less enhanced blue emission. The spectrum of device B is also shown in Fig. 2c. As can be seen from the power distribution of the spectrum of device B and the trend of the cavity emission, we can deduce the spectrum of device A. In Fig. 2c, we also calculated the normal emisson of the device, which is excellent agreement with the experiment results. All of the descriptions above result in the difference of the spectra between devices A and B.

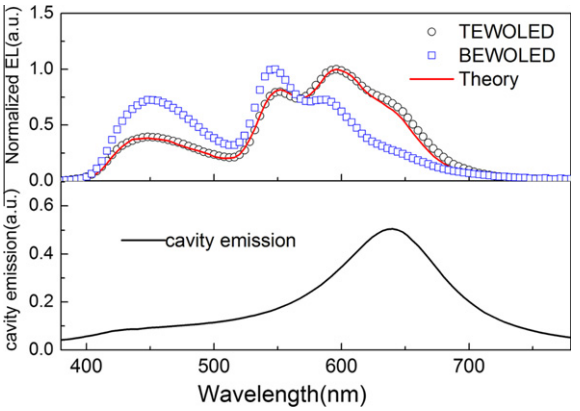

Fig. 2c. The normalized EL spectra by calculating and measuring of the devices (top) and the calculated forward directed cavity emission of device A (down).

Fig. 3 shows the CIE coordinates of devices A and B operated from 5 to 10 V. The CIE coordinates of device A change from (0.3532, 0.3270) to (0.4277, 0.3894) and that of device B change from (0.2562, 0.2689) to (0.323, 0.3533) over all the range of operation voltages. We can see that the CIE coordinates are fairly stable at high operation voltages for the two devices. Besides, the device A has a higher color rendering index (CRI) of 84 at correlated color temperature (CCT) of T_c = 3736 K (Ideal CCT values for warm white is 2500–4500 K [2]) than that of device B (CRI = 75 at T_c = 8224 K), which is an important parameter for lighting sources. This TEWOLED satisfies the CRI need for future solid-state lighting applications (with a CRI > 80) [31].

Fig. 4a shows the current density–voltage–luminance characteristics of the devices, revealing a luminance of 6398 and 6435 cd/m^2 at 9 V for devices A, and B, respectively. When the operating voltage is below 8 V, device A has a lower current density than that of device B. Fig. 4b shows the voltage-efficiency characteristics of the devices. The maximum current efficiency can reach 8.66 and 9.10 cd/A for devices A and B, respectively. We can also see that the MAM-based device has a lower roll-off of efficiency than that of ITO-based one due to the microcavity effect. The microcavity effect increases the optical mode density and consequently increases the radiation rate,

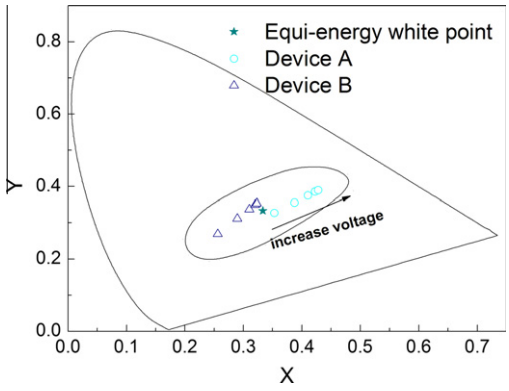

Fig. 3. The CIE coordinates of devices A and B at different operation voltage.

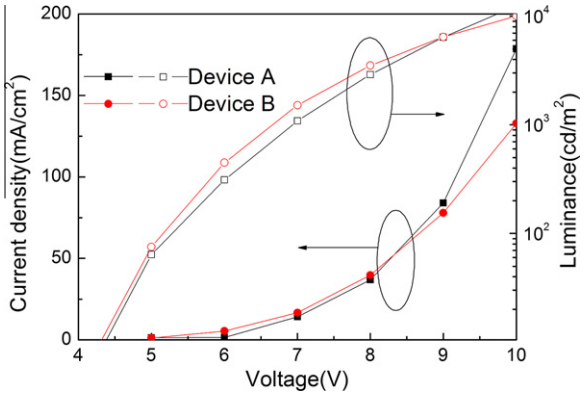

Fig. 4a. The voltage-luminance-current characteristics of the devices.

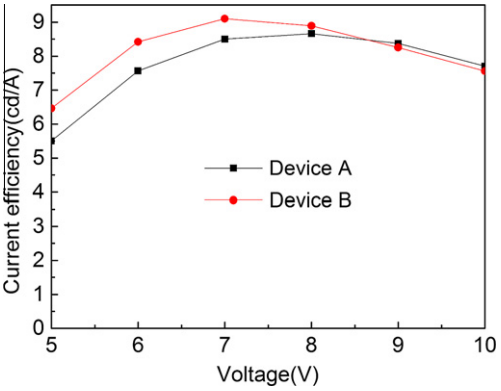

Fig. 4b. The voltage-efficiency characteristics of the devices.

which reduces the possibility of triplet–triplet annihilation [32,33]. However, the TEWOLED exhibits a lower efficiency than that of the ITO-based device. The poor contact and high energy barrier at MAM/organic interface may be two important factors which influenced the performance of MAM-based device. In addition, the thick MoO_3 layer will increase the operating voltage of the devices, as described in Ref. [34], in which thick (>10 nm) MoO_3-doped NPD hole injection layer increased the operating voltage of the device.

4. Conclusions

In summary, we have successfully obtained a warm-white top-emitting organic light-emitting device with MAM multilayer transparent cathode. A high average transmittance of 84% and low resistance of 11 Ω/□ for MAM coatings was obtained. Therefore, the MAM-based electrode structure can be used as a low resistance transparent cathode and anode for transparent or top-emitting OLEDs, especially for flexible devices, in practical applications. Comparing to ITO-based device, MAM-based TEWOLED exhibits some superior performance, such as high CRI and low CCT, which are the key factors to estimating the performance of lighting sources. Most important, the MAM multilayer can be prepared by vacuum thermal evaporation, which is compatible with OLEDs fabrication process.

Acknowledgments

This work was supported by The National Natural Science Foundation of China (Grant Nos. 60937001, 11074096, 61077045, 60723002) and The Ministry of Science and Technology of China (Grant No. 2010CB327701).

References

[1] M.A. Baldo, M.E. Thompson, S.R. Forrest, High-efficiency fluorescent organic light-emitting devices using a phosphorescent sensitizer, Nature (London) 403 (2000) 750.
[2] B.W. D'Andrade, S.R. Forrest, White Organic Light-Emitting Devices for Solid-State Lighting, Adv. Mater. 16 (2004) 1585.
[3] Y.R. Sun, N.C. Giebink, H. Kanno, B. Ma, M.E. Thompson, S.R. Forrest, High-efficiency and color-stable white organic light-emitting devices based on sky blue electrofluorescence and orange electrophosphorescence, Nature (London) 440 (2006) 908.
[4] C.L. Ho, M.F. Lin, W.Y. Wong, W.K. Wong, C.H. Chen, High-efficiency and color-stable white organic light-emitting devices based on sky blue electrofluorescence and orange electrophosphorescence, Appl. Phys. Lett. 92 (2008) 083301.
[5] C.L. Ho, W.Y. Wong, Q. Wang, D.G. Ma, L.X. Wang, Z.Y. Lin, A multifunctional iridium-carbazolyl orange phosphor for high-performance two-element WOLED exploiting exciton-Managed fluorescence/phosphorescence, Adv. Funct. Mater. 18 (2008) 928.
[6] S.J. Su, E. Gonmori, H. Sasabe, J. Kido, Highly efficient organic blue- and white-light-emitting devices having a carrier- and exciton-confining structure for reduced efficiency roll-off, Adv. Mater. 20 (2008) 4189.
[7] S. Reineke, F. Lindner, G. Schwartz, N. Seidler, K. Walzer, B. Lüssem, K. Leo, White organic light-emitting diodes with fluorescent tube efficiency, Nature (London) 459 (2009) 234.
[8] N.T. Salim, K.C. Aw, W. Gao, Z.W. Li, B. Wright, ZnO as a dielectric for organic thin film transistor-based non-volatile memory, Microelectron. Eng. 86 (2009) 2127.
[9] C.H. Li, F. Pan, F. Zhu, D. Song, H. Wang, D.H. Yan, Very low hysteresis organic thin-film transistors, Semicond. Sci. Technol. 24 (2009) 085009.
[10] D.J. Yun, S.H. Lim, T.W. Lee, S.W. Rhee, Fabrication of the flexible pentacene thin-film transistors on 304 and 430 stainless steel (SS) substrate, Org. Electron. 10 (2009) 970.
[11] M. Fischer, M. Nägele, D. Eichner, C. Schö11horn, R. Strobel, Integration of surface-micromachined polysilicon mirrors and a standard CMOS process, Sensor Actuat A: Phys. 52 (1996) 140.
[12] K.A. Honer, G.T.A. Kovacs, Integration of sputtered silicon microstructures with pre-fabricated CMOS circuitry, Sensor. Actuat. A: Phys. 91 (2001) 386.
[13] L.S. Pakula, H. Yang, H.T.M. Pham, P. French, P.M. Sarro, Fabrication of a CMOS compatible pressure sensor for harsh environments, J. Micromech. Microeng. 14 (2004) 1478.
[14] H. Kanno, Y.R. Sun, S.R. Forrest, High-efficiency top-emissive white-light-emitting organic electrophosphorescent devices, Appl. Phys. Lett. 86 (2005) 263502.
[15] S.F. Hsu, C.C. Lee, S.W. Hwang, C.H. Chen, Highly efficient top-emitting white organic electroluminescent devices, Appl. Phys. Lett. 86 (2005) 253508.
[16] M.T. Lee, M.R. Tseng, Efficient, long-life and Lambertian source of top-emitting white OLEDs using low-reflectivity molybdenum anode and co-doping technology, Curr. Appl. Phys. 8 (2008) 616.
[17] M.S. Kim, C.H. Jeong, J.T. Lim, G.Y. Yeom, White top-emitting organic light-emitting diodes using one-emissive layer of the DCJTB doped DPVBi layer, Thin Solid Films 516 (2008) 3590.
[18] W.Y. Ji, L.T. Zhang, T.Y. Zhang, G.Q. Liu, W.F. Xie, S.Y. Liu, H.Z. Zhang, L.Y. Zhang, B. Li, Top-emitting white organic light-emitting devices with a one-dimensional metallic-dielectric photonic crystal anode, Opt. Lett. 34 (2009) 2703.
[19] W.Y. Ji, L.T. Zhang, T.Y. Zhang, W.F. Xie, H.Z. Zhang, High-contrast and high-efficiency microcavity top-emitting white organic light-emitting devices, Org. electron. 11 (2009) 202.
[20] W.Y. Ji, L.T. Zhang, R.X. Gao, L.M. Zhang, W.F. Xie, H.Z. Zhang, B. Li, Top-emitting white organic light-emitting devices with down-

conversion phosphors: Theory and experiment, Opt. Express 16 (2008) 15489.
[21] D.R. Cairns, R.P. Witte, D.K. Sparacin, S.M. Sachsman, D.C. Paine, G.P. Crawford, Strain-dependent electrical resistance of tin-doped indium oxide on polymer substrates, Appl. Phys. Lett. 76 (2000) 1425.
[22] J. Lewis, S. Grego, B. Chalamala, E. Vick, D. Temple, Highly flexible transparent electrodes for organic light-emitting diode-based displays, Appl. Phys. Lett. 85 (2004) 3450.
[23] J.C.C. Fan, F.J. Bachner, H. Foley, P.M. Zavracky, Transparent heat-mirror films of TiO_2/Ag/TiO_2 for solar energy collection and radiation insulation, Appl. Phys. Lett. 25 (1974) 693.
[24] M. Bender, W. Seelig, C. Daube, H. Frankenberger, B. Ocker, J. Stollenwerk, Dependence of film composition and thicknesses on optical and electrical properties of ITO-metal-ITO multilayers, Thin Solid Films 326 (1998) 67.
[25] K.H. Choi, H.J. Nam, J.A. Jeong, S.W. Cho, H.K. Kim, J.W. Kang, D.G. Kim, W.J. Cho, Highly flexible and transparent InZnSnOx/Ag/InZnSnOx multilayer electrode for flexible organic light emitting diodes, Appl. Phys. Lett. 92 (2008) 223302.
[26] H.Q. Pang, Y.B. Yuan, Y.F. Zhou, J.R. Lian, L.F. Cao, J. Zhang, X. Zhou, ZnS/Ag/ZnS coating as transparent anode for organic light emitting diodes, J. Lumin. 122–123 (2007) 587.
[27] K.S. Yook, S.O. Jeon, C.W. Joo, J.Y. Lee, Transparent organic light emitting diodes using a multilayer oxide as a low resistance transparent cathode, Appl. Phys. Lett. 93 (2008) 013301.
[28] S.Y. Ryu, J.H. Noh, B.H. Hwang, C.S. Kim, S.J. Jo, J.T. Kim, H.S. Hwang, H.K. Baik, H.S. Jeong, C.H. Lee, S.Y. Song, S.H. Choi, S.Y. Park, Transparent organic light-emitting diodes consisting of a metal oxide multilayer cathode, Appl. Phys. Lett. 92 (2008) 023306.
[29] C.L. Mitsas, D.I. Siapkas, Generalized matrix method for analysis of coherent and incoherent reflectance and transmittance of multilayer structures with rough surfaces, interfaces, and finite substrates, Appl. Opt. 34 (1995) 1678.
[30] P. Freitag, S. Reineke, S. Olthof, M. Furno, B. Lüssem, K. Leo, White top-emitting organic light-emitting diodes with forward directed emission and high color quality, Org. Electron. 11 (2010) 1676.
[31] S. Nizamoglu, G. Zengin, H.V. Demir, Color-converting combinations of nanocrystal emitters for warm-white light generation with high color rendering index, Appl. Phys. Lett. 92 (2008) 031102.
[32] M.A. Baldo, C. Adachi, S.R. Forrest, Transient analysis of organic electrophosphorescence. II. Transient analysis of triplet-triplet annihilation, Phys. Rev. B 62 (2000) 10967.
[33] S. Reineke, K. Walzer, K. Leo, Triplet-exciton quenching in organic phosphorescent light-emitting diodes with Ir-based emitters, Phys. Rev. B 75 (2007) 125328.
[34] S.W. Cho, L.F.J. Piper, A. DeMasi, A.R.H. Preston, K.E. Smith, K.V. Chauhan, R.A. Hatton, T.S. Jones, Soft X-ray spectroscopy of C60/copper phthalocyanine/MoO_3 interfaces: role of Reduced MoO_3 on energetic band alignment and improved performance, J. Phys. Chem. C 114 (2010) 18252.